Comparison of embolic effects between permanent and novel resorbable microspheres in a porcine renal artery embolization model for TAE

Sankalp Agarwal*§†, Masum Pandey§, Ronan Duggan† , Con O' Brien† , Andrew. L. Lewis† , Brendan Duffy§ , Joan McCabe† , and Liam Farrissey*† .

§ Centre for Research in Engineering and Surface Technology, TU Dublin, Ireland.

† CrannMed Ltd, Galway, Ireland

*Email: sankalp.agarwal@crannmed.com

*Email: Liam.Farrissey@Crannmed.com

Abstract:

Embolotherapy has been widely practised for musculoskeletal (MSK) pain relief applications. It involves the intentional occlusion of blood vessels to reduce or prevent blood flow to target regions or organs using a vascular embolic agent. This study evaluated renal artery embolization using resorbable microspheres (SakuraBead, RM) compared to permanent microspheres (Embozene, PM) in Yorkshire swine, assessing vessel occlusion duration, local and systemic reactions, and potential adverse effects. Angiography was performed to confirm successful stasis at all injection sites. Clinical observations, body weights, and pathology were monitored at regular intervals, and animals were euthanized at 24 hours, and on Days 3, 7, and 28 for necropsy and histomorphometric analysis. Results showed that all animals survived without significant adverse effects, maintaining body weight and condition. No significant hematologic or serum chemistry abnormalities were observed, except for transiently elevated activated partial thromboplastin time in five animals' post-treatment. Macroscopically, treatment-related findings were minimal in the RM group and more pronounced in the PM group. Histologically, RM was rarely observed beyond 24 hours, with negligible inflammation and vascular injury. In contrast, PM persisted, accompanied by mild inflammation and vascular injury extending to the tunica media or adventitia. No systemic tissue responses were detected in either group. This study demonstrated that RM provides effective, transient embolization with minimal local or systemic adverse effects, making it suitable for indications such as genicular artery embolization, tendinopathy, and adhesive capsulitis, where temporary vessel occlusion is required.

1 INTRODUCTION

Embolotherapy is a widely practiced minimally invasive vascular intervention, involving intentional occlusion of one or more vessels to reduce or prevent blood flow to a target region or organ. It is used to treat conditions such as hemorrhage, a variety of vascular anomalies, benign tumors and certain solid cancers. Central to the success of the procedure is a thorough understanding of the clinical application, the technical skill of the treating physician and the correct selection of the most appropriate embolic agent for the treatment in question. There is an impressive array of embolic devices available from which to choose, including metallic coils, temporary and permanent particulate materials/microspheres and liquid agents that sclerose, solidify or polymerize within the vessel. Particulate embolic agents in particular, offer a high degree of flexibility as they can be prepared, or are generally available, in size ranges that can be. The most used temporary embolic is Gelfoam®, a gelatin-based sponge or powder indicated for hemostasis, that is manually formed by physicians into pledgets or particle slurries for off-label intraarterial embolization (Camacho et al., 2019). Many alternative polymer-based degradable embolic systems have been described in the literature, for instance, based upon materials such as polyethylene glycol-polylactic/glycolic acid copolymer (PEG-PLGA-PEG) (Maeda et al., 2013), carboxymethyl cellulose / chitosan (Weng et al., 2011), albumin and hydroxyethyl acrylate (Schwarz et al., 2004). Relatively few have progressed to even preclinical evaluation (Doucet et al., 2018), although a number of degradable microspherical embolization products are now commercially available. The longest established product is based upon degradable starch microspheres (DSM, Embocept®, Pharmacept GmbH) which offers a temporary disruption of blood flow for around 30-40 minutes before being rapidly broken down by a-amylase in plasma (Pieper et al., 2015), somewhat limiting its use. The other products are based on gelatin (X-Pure® Embolic Gelatin, Rousselot Biomedical) or poly(lactic-co-glycolic) acid (Ekobi® [formerly Occlusin] IMBiotechnologies Ltd). Neither has yet seen wide-spread adoption in embolotherapy, as degradation is somewhat unpredictable or lengthy in time frame (Owen et al., 2012), as it is dependent upon a combination of hydrolytic and enzymatic degradation that is influenced by multiple factors, such as extent of embolization, the location embolized, influence of mechanical effects and the biological variation between patients. It is therefore unlikely that in the case of embolic degradable microspheres there

will be a “one size fits all” solution, rather products will need to be engineered with properties that befit the specific clinical indication.

Alginate is a highly abundant naturally occurring polysaccharide derived primarily from brown seaweed, that has been investigated extensively for applications in biomedical engineering including wound care (M. Zhang & Zhao, 2020), hemostasis (Xie et al., 2022), drug delivery (Jain & Bar-Shalom, 2014), cell encapsulation (Simó et al., 2017), cancer therapy (Reig-Vano et al., 2021) and embolotherapy (Becker et al., 2000). It is not one specific material but rather a family of linear copolymers containing blocks of (1,4)-linked b-mannuronate [M] and a-L-guluronate [G] residues, the latter participating in ionic crosslinking with divalent cations (most commonly Ca^{2+}) to form hydrogels. The physical properties of alginate hydrogels can therefore be exquisitely controlled by variations in M:G ratio, G-block length, molecular weight and choice of divalent cation (H. Zhang et al., 2021). In their purified form, alginates are highly biocompatible and can be fabricated into hydrogel implants that remain stable within the body for years (Forster et al., 2010), as there is no enzyme in humans for which alginate is a substrate and hydrolytic cleavage of the glycosidic bond is a slow process. The facile gelation of alginate using divalent cation crosslinking has prompted interest in alginate for both *in-situ* endovascular embolization (Barnett et al., 2009; Becker et al., 2000)and for microspherical embolic agents with encapsulated drugs (Van Elk et al., 2015) and imaging agents (Zeng et al., 2018).

Given its stability *in vivo*, alginate may not present itself as an ideal choice as a platform for the development of a range of tailored degradable microspherical embolic products. Others have shown, however, that alginate embolic agents can be selectively degraded on demand *in vivo* by intraarterial administration of either calcium sequestration agents (Choi et al., 2021) or by the application of alginate lyase enzyme within the embolized vessel (Barnett et al., 2009). This proffers the attraction of reversing the effects of the embolic agent in the case of emergency, for instance rescuing the effects of off-target placement of the embolic. Moreover, if alginate lyase could be incorporated and stabilized within the alginate embolic agent and activated upon administration into the body, it could provide a route to controlled self-degradation of the embolic that would be completely independent of the factors responsible for the variable degradation rates observed for the existing products. SakuraBead is just such a product that has been engineered in the first instance for

treatment for osteoarthritis of the knee involving selective genicular artery embolization (GAE) and potentially other tendinopathies where temporary local ischemia has been shown to bring pain relief (Torkian et al., 2021). The most impressive results to date involving this procedure have been achieved using an off-label embolic mixture obtained by placing the antibiotic combination of imipenem and cilastatin in saline:contrast to generate crystalline particles of 1-50 microns in size that degrade and re-establish flow over around a 2 hour time period (Bhatia et al., 2023; Okuno et al., 2015). Alginate microsphere degradation properties were tuned by selection of M:G ratio, molecular weight and incorporated alginate lyase concentrations to obtain a self-degrading microspherical embolic product with a degradation profile and clinical imaging outcome comparable to imipenem:cilastatin (IMP/CS) suitable for application in GAE. Herein we describe the safety and embolization effects of the resorbable SakuraBead in comparison with Embozene permanent embolic particles.

2 MATERIALS AND METHODS

Animal Model and Husbandry

The healthy swine model was chosen as the experimental species for these studies because the size and anatomy of the peripheral vascular system is clinically relevant for the purpose of testing peripheral vascular medical devices. Animals were housed under conditions that met or exceeded requirements as set forth in the USDA AWA/AWR and as described in the Guide. Environmental conditions (temperature, relative humidity, and light) within the animal facility were monitored. There were no variations from the ranges outlined in the Guide that were considered to have negatively affected animal well-being, research performance, or the results and outcomes of the study. Swine were offered Purina Lab Diet (#5084 Laboratory Porcine Diet Grower) once daily and potable water was provided *ad libitum* to all animals. This study is conducted in compliance with the Food and Drug Administration GLPs, as set forth in Title 21 of the United States CFR, Part 58. The IACUC Project Number for this study is I00362 (Global Protocol).

Study Design

Twelve Yorkshire swine (n=3 Female, n=9 Male) underwent a single interventional procedure on Day 0 in which a discrete portion of one pole of each kidney was embolized with either the RM or the PM, as outlined in Table 1. Angiography was performed and recorded before and after the embolization treatment, then ~5-10 minutes after the last embolization treatment. Animal health, including clinical observations, body weights/condition, and clinical pathology were generally monitored at pre-determined, regular intervals. Animals were euthanized at 24 hours, Days 3, 7, and 28 post treatment and subjected to a comprehensive necropsy. The kidneys were removed in toto, photographed, and fixed with 10% NBF. Treated and untreated kidney tissue was processed for histopathological evaluation. Additionally, representative tissue samples of brain, heart, liver, lung, and spleen were collected and processed for histopathological evaluation (scheme 1 and table 1).

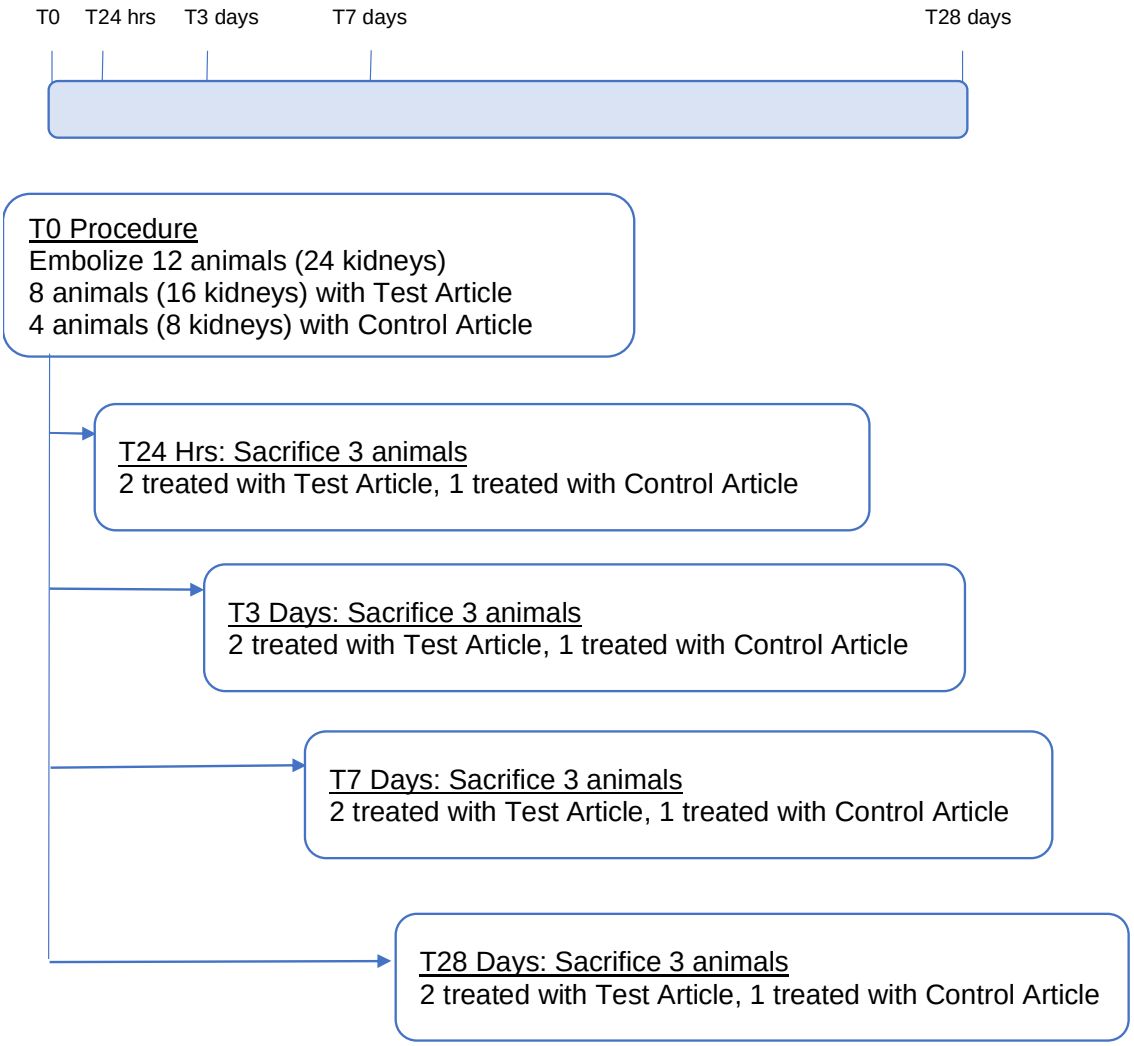

Scheme 1 showing the detail protocol of study

Table 1: Study Design Outline

Treatment Group	Number of Animals	Description of Treatment	Number of Treatments per Animal	Necropsy Timepoint
1	2	Kidney injection with RM	2	24 Hours
	1	Kidney injection with PM		
2	2	Kidney injection with RM	2	Day 3
	1	Kidney injection with PM		
3	2	Kidney injection with RM	2	Day 7
	1	Kidney injection with PM		
4	2	Kidney injection with RM	2	Day 28 ± 1
	1	Kidney injection with PM		

Anaesthesia and Perioperative Procedures

Animals were not offered their daily food ration prior to surgical induction to decrease the chances of perioperative vomiting or regurgitation. Water was not restricted. Daily food ration was provided upon recovery from anaesthesia. Tiletamine-zolazepam (4-6 mg/kg, IM) was administered as a pre-anaesthetic. Isoflurane anaesthesia (delivered in 100% oxygen) was administered to effect via mask/nosecone until the animals were in a plane of anaesthesia that facilitated endotracheal intubation. Once sufficiently anesthetized, the animals were intubated and maintained on continuous inhalant isoflurane anaesthesia delivered to effect in 100% oxygen for the remainder of the procedure. Perioperative nifedipine (10 mg/animal placed sublingually) was administered. An IV catheter was placed in a peripheral vein for administration of supportive IV fluids. An ophthalmic lubricant was applied to the eyes. The animals were prepared for surgery using accepted veterinary care standards. Pre-emptive analgesia, buprenorphine (0.01 mg/kg, IM), was administered at time of anaesthesia/surgical induction (prior to surgical incision). The animals were placed in dorsal recumbency to facilitate the surgical procedure. Supportive fluids were administered and the fluid type and volume administered was documented in the animal's record. Warm

water heating pads and/or other warming devices were used to help maintain adequate body temperature while under anaesthesia. The incision site was prepared and appropriately draped for aseptic procedures.

Vascular Access and Anticoagulation Monitoring

After induction of anaesthesia, an incision was made in the inguinal region to expose the right femoral artery. An introducer sheath was advanced into the artery and heparin (150-200 U/kg, IV) was administered to prolong ACT to a target of minimally 200 seconds. Blood samples (< 0.5 mL each) were collected within 5-10 minutes of heparin administration. Once the ACT value had reached the target, additional tests were run within 45 minutes of the previous test/sample. Additional heparin (50 U/kg, IV) was administered as needed to maintain the target ACT.

Interventional Procedures

Under fluoroscopic guidance, an appropriately sized guide catheter was advanced through the sheath over a guidewire to the renal arteries. Angiographic images of the vessels (with and/or without subtraction) were obtained with contrast media to identify the proper location for treatment. Nitro-glycerine (200 µg, IA) was administered when needed to treat vasospasm. Once at the target site, a microcatheter was advanced through the guide catheter. One embolization treatment was performed in each kidney for both studies.

For the PM group, embolic microspheres were delivered through the microcatheter in consideration of the respective IFU supplied with the product (100 mm Embozene® Microspheres, Varian Medical Systems, Palo Alto, California). Generally, the embolization procedure was as follows: The contents of the prefilled syringe were gently swirled before the syringe was opened and a mixture of 50% contrast agent and 50% saline was added to the product syringe (i.e., 5 mL contrast and 5 mL saline). The syringe was gently swirled every 30 seconds until a homogenous suspension was achieved and gently swirled to re-suspend before delivery, if required. All air was purged from the 20 mL syringe which was attached to one port of the luer-lock 3-way stopcock and a 1 mL injection syringe was attached to another port of the stopcock. The remaining port of the stopcock was attached

to the high flow microcatheter. The microspheres were drawn slowly and gently into the injection syringe. Under continuous fluoroscopic guidance, microspheres were slowly infused *via* pulsatile injection (~0.1 mL at a time) into the blood stream. Infusion was continued until the desired volume was delivered to achieve stasis. Once the desired endpoint was reached, a waiting period of 5-10 minute was allowed to observe whether the microspheres redistributed themselves and re-established flow to the target. If flow was re-established, additional microspheres were injected until stasis was achieved.

For RM, microspheres were delivered through the microcatheter in consideration of the respective IFU supplied with the product (200 mm SakuraBead, CrannMed Ltd, Ireland) and was as follows: 1.5 mL saline was added to the contents of the vial and a period of ~ 2 mins was allowed for the contents of the vial to dissolve, or until the solution was completely clear. The vial was swirled to aid dissolution and 2 mL of non-ionic contrast agent was added into the vial. The vial was gently inverted several times to mix the solutions. A needle (21-gauge or larger) was attached to a 3 mL syringe and the vial was inverted to disperse the microspheres in the solution. The needle was inserted into the vial and the microsphere solution was gently aspirated into the syringe, after which the needle was removed, and the syringe was attached to the microcatheter. Under continuous fluoroscopic guidance, microspheres were slowly infused *via* pulsatile injection (~0.1 mL at a time) into the blood stream. Infusion was continued until the desired volume was delivered to achieve stasis. Once the desired endpoint was reached, a waiting period of 5-10 minute was allowed to observe whether the microspheres redistributed themselves and re-established flow to the target. If flow was re-established, additional microspheres were injected until stasis was achieved. Fluoroscopy was used to qualitatively evaluate parameters such as vascular anatomy, treatment site suitability, and/or acute deployment characteristics. Subtracted and/or unsubtracted angiograms were recorded immediately before and after the procedure and 5-10 minutes after the last embolization treatment. The angiograms were recorded in digital format and transferred to digital storage media.

At the conclusion of the procedure, the accessed vessel was ligated. Bupivacaine was administered (0.36-0.47 mg/kg, SC) at the incision site and the surgical incision was closed with appropriate suture techniques and materials. Electrocardiogram, heart rate, respiratory rate, SpO2, temperature and direct blood pressure were monitored and

documented at regular intervals during the surgical procedure. Positive pressure mechanical ventilation was used when needed during the anesthetic procedure. Any animal placed on mechanical ventilation was gradually weaned off ventilatory support and continuously monitored and supported with manual ventilation (if needed) until spontaneous respirations resumed. Animals were continuously monitored until endotracheal extubation occurred. The animals were extubated and post-operative care procedures were performed in accordance with accepted veterinary standards. Animals were monitored until recovered fully from anesthesia. Buprenorphine (0.01 mg/kg, IM) was administered minimally every 12 hours to provide analgesic coverage through the first 24 post-operative hours.

Euthanasia and Necropsy

Where tissue samples were to be collected, animals were administered tiletamine-zolazepam (4 mg/kg, IM) and anesthetized via isoflurane inhalant. An IV catheter was placed in a peripheral vein. Heparin (200 U/kg, IV) was administered followed by an overdose of potassium chloride (2 mEq/kg, IV) in accordance with accepted AVMA guidelines. A comprehensive necropsy was conducted on all animals. The necropsy included examination of all external surfaces and orifices, and the cranial, thoracic, abdominal cavities and contents. The kidneys were removed *in toto*, photographed, and immersion fixed with 10% neutral buffered formalin (NBF). Prior to fixation, the untreated portions of the kidneys were breadloafed (without separating the breadloafed sections) to allow for complete fixation. Representative samples from non-target organs were collected and placed in 10% NBF.

Blood Sampling and Analysis

Blood samples were collected from a peripheral vessel at Day 0 prior to surgery, 15 1 mins after the last embolization treatment and on the day of necropsy. Whole blood hematology samples were maintained under ambient conditions until analyzed by CBSET. A blood smear was made and whole blood samples were analyzed for a range of hematology parameters. After collection, samples for coagulation were processed for plasma, then stored frozen until shipment on dry ice. All samples were shipped by overnight courier to the clinical

pathology facility for analysis. The plasma was analyzed for fibrinogen, prothrombin time and activated partial thromboplastin time. Samples for serum chemistry were processed for serum then stored frozen until shipment on dry ice. All samples were shipped by overnight courier to the clinical pathology facility for analysis. Serum samples were analyzed for a wide range of serum chemistry parameters.

Histology and Histomorphometry

Macroscopic photography was obtained during trimming to document and assist in maintaining orientation of trimmed tissue. Treatment areas were identified via interventional data, in vivo imaging, or other means. The kidneys were sampled at the proximal, middle, and distal treated region and at two sites of the untreated kidney region. Trimmed specimens were paraffin-embedded and stained with H&E. Histopathological evaluation was performed *via* assessment of glass slides. Light microscopy was used to examine sections of treated kidney and associated tissue for any changes associated with treatment or reparative/regenerative response. Evaluation included parameters related to vascular findings (injury, endothelial loss, occlusion), treatment material (presence, degradation), local tissue responses (inflammation, necrosis, fibrosis, and mineralization). Values and/or observations obtained from the histomorphologic analysis were entered into a Microsoft Excel spreadsheet. Ordinal histologic data (scores) were reported as the group median, mean ± SD, and percent incidence, as appropriate. Group calculations were performed using rounded values and reported rounded to 2 decimal places with the exception of percent incidence (reported as a whole number). Calculations, data organization, and the graphs were generated using Excel® for Microsoft 365 software.

3 RESULTS

Device Deployment, Clinical Observations and Clinical Pathology

Representative angiographic images are shown in Figure 1 (A-D) and in 100% of cases the desired targeted segment of the kidney was devascularized. All sites according to the study design in Table 1 were successfully embolized with the RM and PM on Day 0, as stasis was achieved in the targeted vasculature of all treatment sites. In some cases, multiple applications of the products were required to achieve stasis and on 4 occasions (2 RM and 2

PM) some reflux was observed that resulted in a small degree of off-target embolization in 3 instances. There was no early mortality; all animals survived the procedure and were euthanized at their pre-determined endpoint. All animals maintained or gained weight and maintained body condition throughout the course of the study, as anticipated. Multiple animals (10 of 12) had right hind limb lameness, manifesting as toe-touching and/or knuckling behavior, on Day 0 which was presumed to be a sequela of the right femoral artery vascular access procedure. All these cases had resolved by Day 1. No significant findings were noted in hematology and serum chemistry results for any of the animals enrolled in this study. Elevated activated partial thromboplastin time (APTT) was observed in 5 out of 12 animals only at the 15 minutes post treatment time point. This elevation was most likely due to heparin administered during the interventional procedure. All other coagulation parameters were within normal limits.

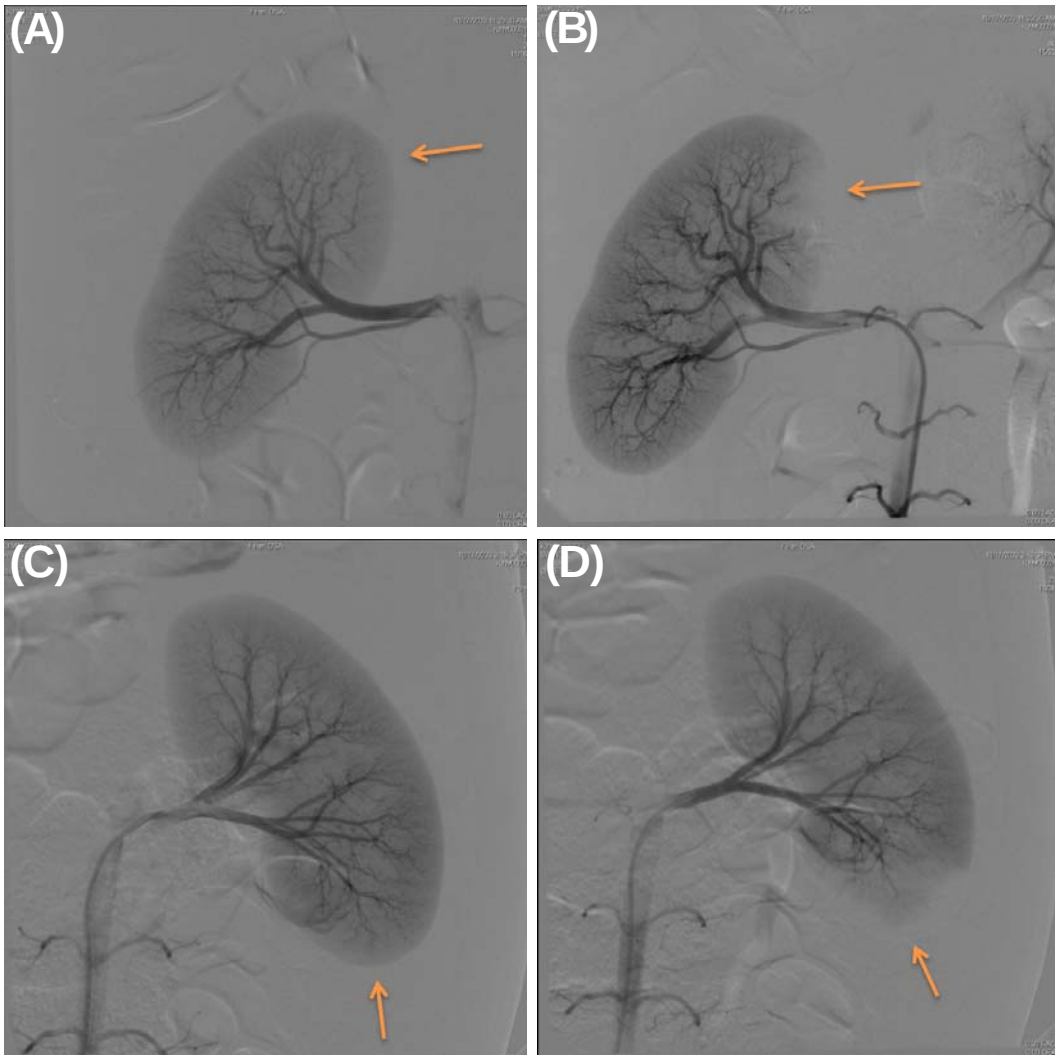

Figure 1: *Representative angiograms (A) Right cranial renal artery, before treatment with RM; (B) immediately post-treatment with RM. (C) Left caudal renal artery, before treatment with PM; (D) immediately post-treatment with PM.*

Gross Necropsy Observations

Macroscopic observations at necropsy, related to treatment, were limited to the kidneys. These were absent to mild in the RM group (Fig. 2 (A-D)) and consistent and notable in the PM group and (Fig. 2 (E-H)). Each PM group animal at all time points exhibited regionally extensive bilateral, acute to chronic renal infarction characteristic of a sustained ischemic insult of the tissue.

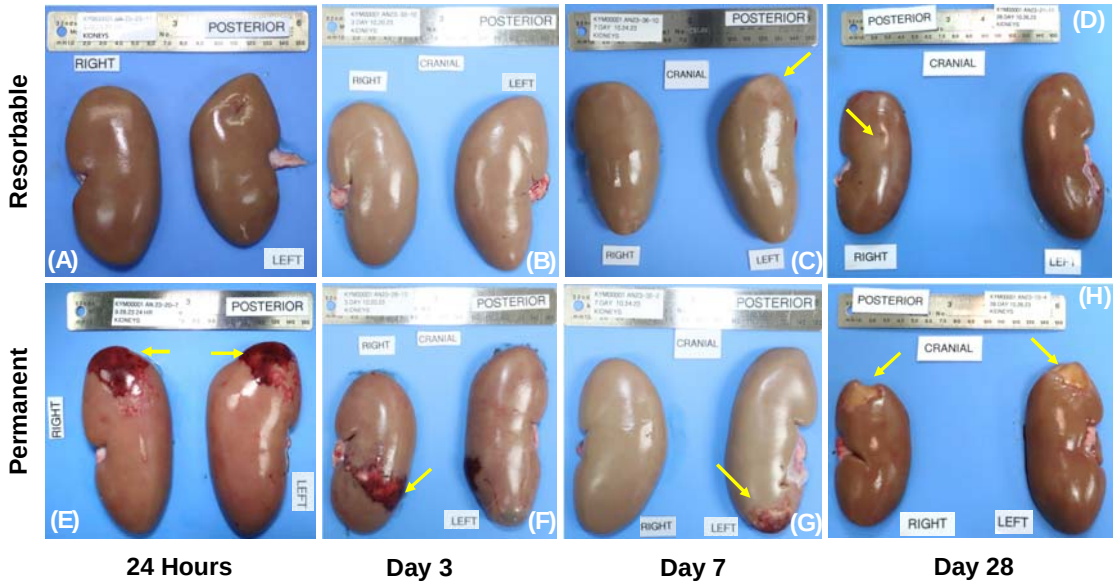

Figure 2: *Gross pathological examination of the kidneys following necropsy. Top row RM group: (A) 24 hours (no gross findings); (B) Day 3 (pale focus (3 x 1 cm) on the cranial pole of the left kidney, corresponding to mixed histologic changes referable to treatment: multifocal interstitial infiltrates, fibroplasia, superficial cortical fibrosis, and tubular degeneration/regeneration); (C) Day 7 (Bilateral tan/brown discoloration (left kidney cranial pole (yellow arrow); 2 x 1 cm, and right kidney caudal pole 2 x 0.5 cm) at necropsy, though these foci were not seen in images of post-fixed tissues);(D) Day 28 (no gross findings).*

Bottom row PM group: (E) 24 hours: Bilateral dark purple/red discoloration on the cranial pole of both kidneys (yellow arrows), histologically corresponding to regionally extensive acute infarction caused by PM); (F) Day 3 (Bilateral red/purple areas near the caudal pole (5 x 2.5 cm right (yellow

arrow) and 3.5 x 3.5 cm left). These corresponded with regionally extensive acute infarction due to arterial occlusion by PM; (G) Day 7 (Bilateral dark discoloration (left kidney caudal pole; 4 x 2.5 cm (yellow arrow), and right kidney caudal pole 4 x 2 cm). These corresponded with regionally extensive, localized chronic infarction due to arterial occlusion by PM); Day 28 (Bilateral sunken tan/brown discoloration (yellow arrows, each 2 x 3 cm). These corresponded with regionally extensive chronic infarction due to arterial occlusion by PM).

Histomorphology Observations

Figure 3(A-C) summarise the main observations from the histomorphology results. Representative microscopic images of histology slides for RM and PM treated animals at 24 hours and 28 days are shown in Figure 4. Histopathologic assessment of systemic tissues included heart, brain, liver, lung and spleen (not presented graphically, see Appendix 3 for individual scores). There were no findings attributable to treatment material in either the RM or PM groups, regardless of time point. Findings were restricted to uncommon incidences of minimal to mild findings typical of incidental/background findings in experimental swine.

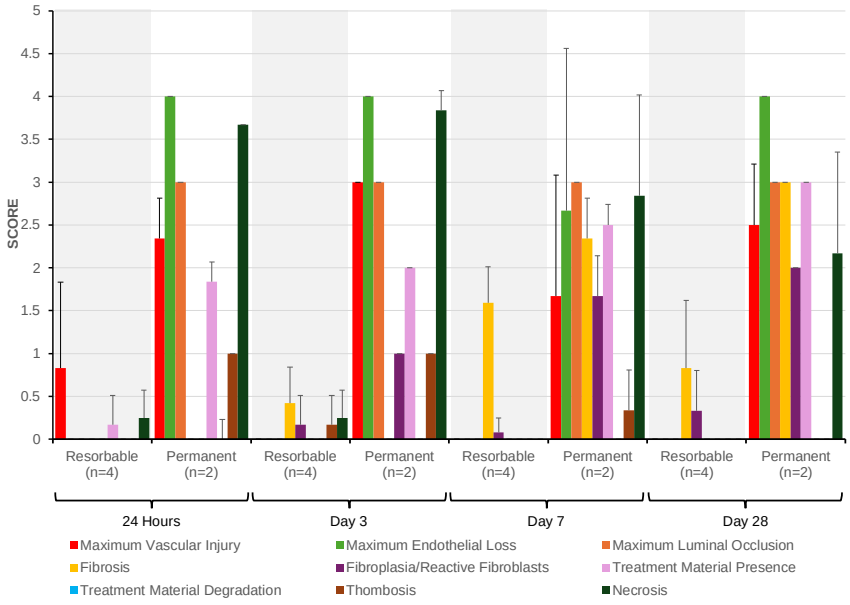

Figure 3: *(A) Histomorphology observations of intrinsic vascular responses: s and Day 3, where it was occasional (50% incidence) and minimal (mean 0.25).*

In the PM group renal cortical necrosis was universally present across time points, being widespread and marked (mean 3.67-3.84) at 24 hours and Day 3, and subsequently decreased to moderate (mean 2.84) at Day 7 and mild (mean 2.17) at Day 28. Mineralization (e.g., typically resulting from epithelial degeneration or necrosis) in the RM group was limited to negligible (mean 0.17) presence at Day 7. In the PM group it was absent through Day 3, mild (mean 2.00) at Day 7 and minimal (mean 0.17) at Day 28. Tubular epithelial vacuolation (consistent with non-lethal cellular injury) decreased in both groups from mild at 24 hours (mean 1.67-1.84) to absent at Day 7 and Day 28. Tubular epithelial degeneration/regeneration (as evidenced by cellular changes including cytoplasmic basophilia) was minimal in RM groups across time points (peak of mean 1.25 at Day 7), while it increased to moderate (mean 3.00) in PM groups at Days 7 and 28. Tubular hyaline casts (indicative of tubular protein accumulation) decreased from minimal in RM groups at 24 hours and Day 3 (mean 0.34-0.58) to absent or nearly so at Day 7 and Day 28 (mean ≤0.08), while they were consistently minimal (mean 0.67-1.00) in PM groups across time points.

Intrinsic Vascular Responses:

Luminal occlusion was not seen in the RM group, regardless of time point, while maximum luminal occlusion in the PM group was marked across time points (mean 3.00; >75% occlusion). Thrombosis was absent or nearly so in the RM groups (mean 0.17 and 25% incidence at Day 3 only). It was uniformly present, though minimal (mean 1.00), in PM groups at 24 hours and 3 days, and subsequently decreased to absent at Day 28. Endothelial loss was not seen in the RM group, regardless of time point. Maximum endothelial loss in the PM group was marked at most time points (mean 4.00; < 25% endothelial coverage) and moderate (mean 2.67; 50 to 25% luminal surface coverage) at Day 7. Maximum vascular injury was uncommon and restricted to the tunica media (with mean score 0.83) in the RM group at 24 hours and absent at all subsequent time points. Vascular injury (i.e., disruption of the arterial wall) in the PM group generally extended to tunica media or EEL/adventitia (mean 1.67-3.00) regardless of time point.

Local Tissue Responses:

Haemorrhage was not seen in the RM group, while in the PM group it decreased progressively from moderate at 24 hours and Day 3 (mean 2.67-3.00) to absent at Day 28. Fibrosis (i.e., presence of mature collagen as part of a chronic tissue response) was not seen with either group at 24 hours. At Day 3 fibrosis was absent in the PM group and minimal

(mean 0.42) in the RM group. At Day 7 it was mild (mean 2.34) in the PM group and minimal-mild (mean 1.59) in the RM group. At Day 28 it was moderate (mean 3.00) in the PM group and minimal (mean 0.83) in the RM group. Fibroplasia (i.e., presence of reactive fibroblasts as part of a subacute to chronic response) were not seen with either group at 24 hours. At Day 3 it was minimal in the PM group (mean 1.00) and nearly absent (mean 0.17) in the RM group. At both Day 7 and Day 28 fibroplasia was mild in the PM group (mean 1.67-2.00) and nearly absent in the RM group (mean 0.08-0.33). Neovascularization was not seen in either group at any time point except the Day 28 PM group, where it was minimal (mean 1.17). Cortical and medullary interstitial lymph histiocytic infiltrates, representing a chronic inflammatory presence, are a common, incidental background finding in experimental swine, and also can be present due to tissue injury or necrosis. In untreated sections these infiltrates were nearly always absent or minimal across time points (with rare mild scores).

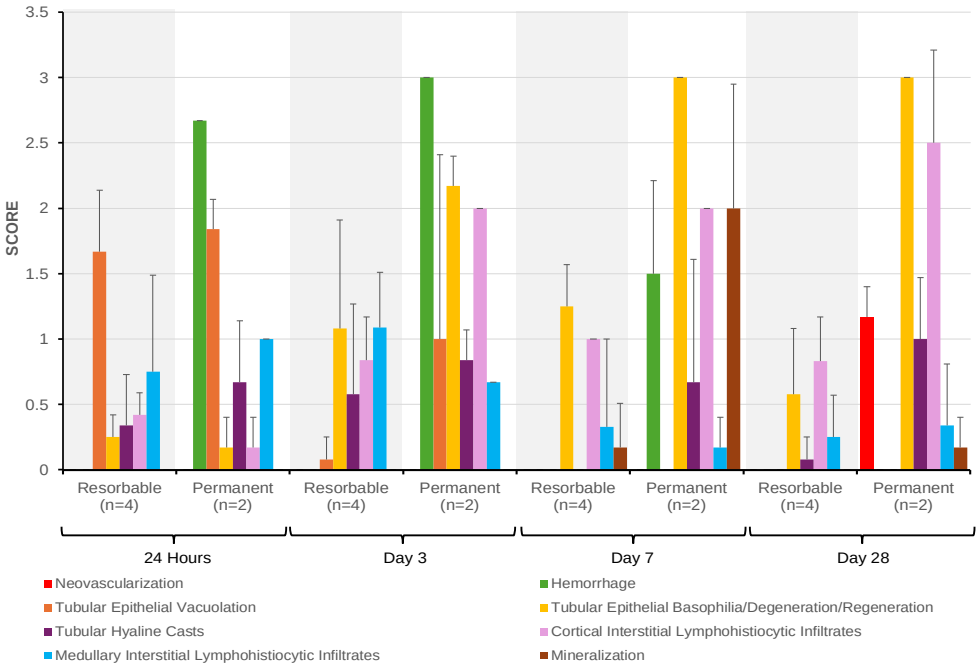

Figure 3: (B) Histomorphology observations of renal epithelial related findings and local tissue responses

Inflammatory Response

There was no inflammation noted in untreated kidney sections. There was no treatment material-associated inflammation in the RM group, regardless of time point. Treatment material-associated inflammation in the PM group was overall minimal or minimal-mild across time points (mean 1.00-1.67) with neutrophils predominant through Day 3 and macrophages and giant cells at Days 7 and 28.

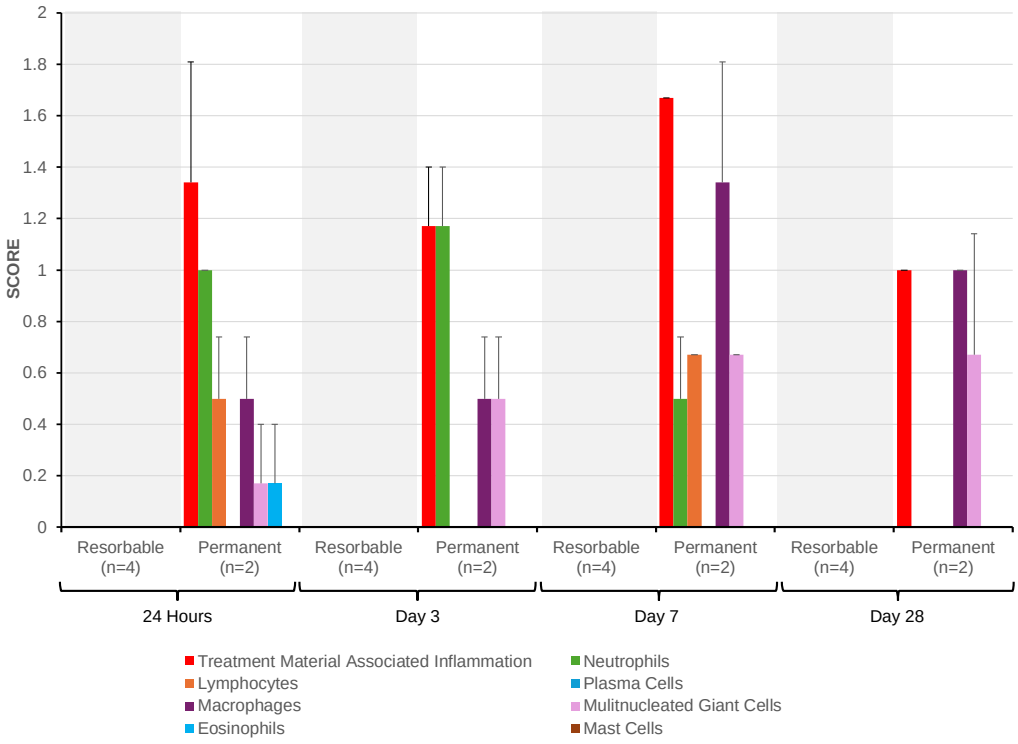

Figure 3(C): Histomorphology observations of inflammatory response

Histology observations- Presence of Embolic Material:

In the RM group, findings consistent with residual embolic material were only identified at 24 hours, being uncommon (25% incidence, i.e., 1 of 4 animals), inconspicuous (isolated single foci of possible material in two renal sections) and overall negligible (i.e., nearly absent/mean 0.17 across animals at 24 hours, Figure 4 A-B). For the PM group, embolic material presence was readily apparent and consistent across all time points (mean 1.84-2.00 at 24 hours and 3 days, mean 2.50 at 7 days and mean 3.00 at 28 days, Fig. 4 C, D, H & I). No degradation (e.g., evidence of bioresorption or biomodification) of either embolic

material was evident. Furthermore, the histology observation of treated kidney sections at subacute to chronic time points (i.e., from Day 3 onwards), and such inflammation was nearly always absent or minimal in the RM group (rare mild scores) while it was very often mild to mild-moderate in the PM group, consistent with response to ischemic injury/infarction. Cumulative renal tissue responses associated with the administration of the RM material were indicative of dispersed, minute areas of ischemic injury at the level of glomerular capillaries while showing signs of regenerative process at 28 days (Fig. 4(G)). PM material was associated with regionally extensive, localized regions of transcortical (i.e., glomerular, tubular and interstitial) infarction with abundant intraarterial microspheres present across time points (Fig. 4 (C,D & H,I).

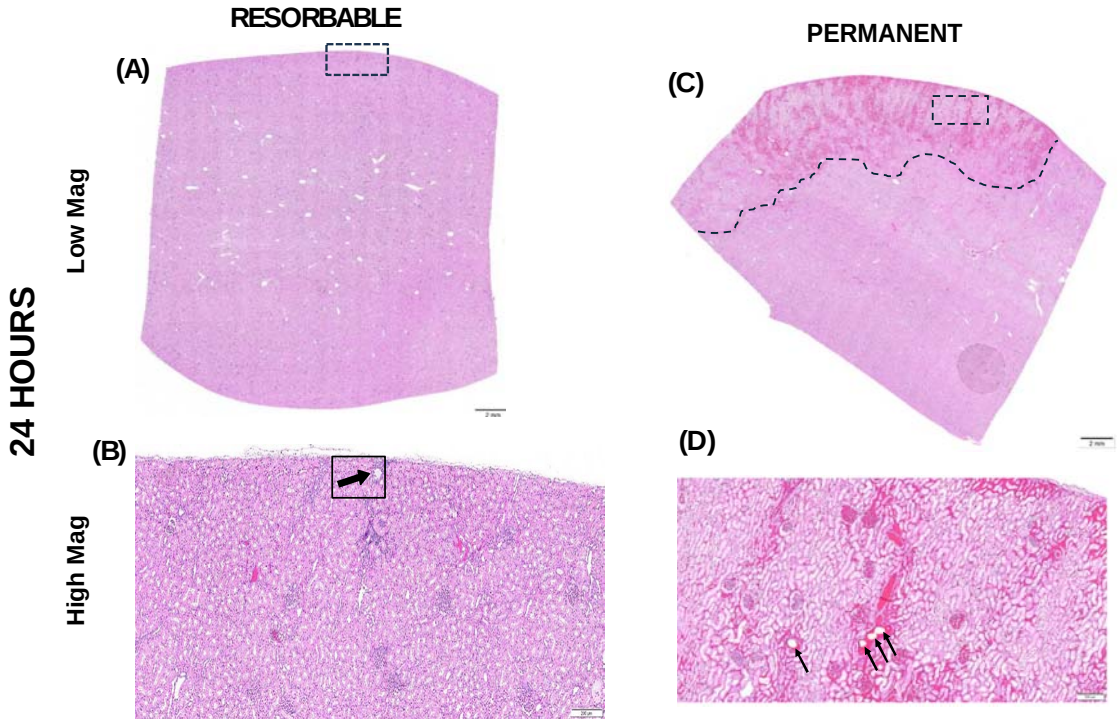

Figure 4 (A-D): (A) Low magnification view (scale bar 2mm) of a section of the right kidney treated with RM after 24 hours; (B) Higher magnification image (scale bar 200 µm) of box in (A) shows a

single focus (arrow) of suspected RM embolic material without any associated tissue responses indicates the fragment is around 40 mm in diameter). (C) Low magnification view (scale bar 2mm) of a section of the left kidney treated with PM after 24 hours showing extensive focus of cortical necrosis indicated by the dashed line; (D) High magnification view (scale bar 200 µm) of box in (C) shows a broad region of acute cortical tubular, glomerular and interstitial necrosis (diffusely throughout this field) with hemorrhage. Several PM are indicated with black arrows.

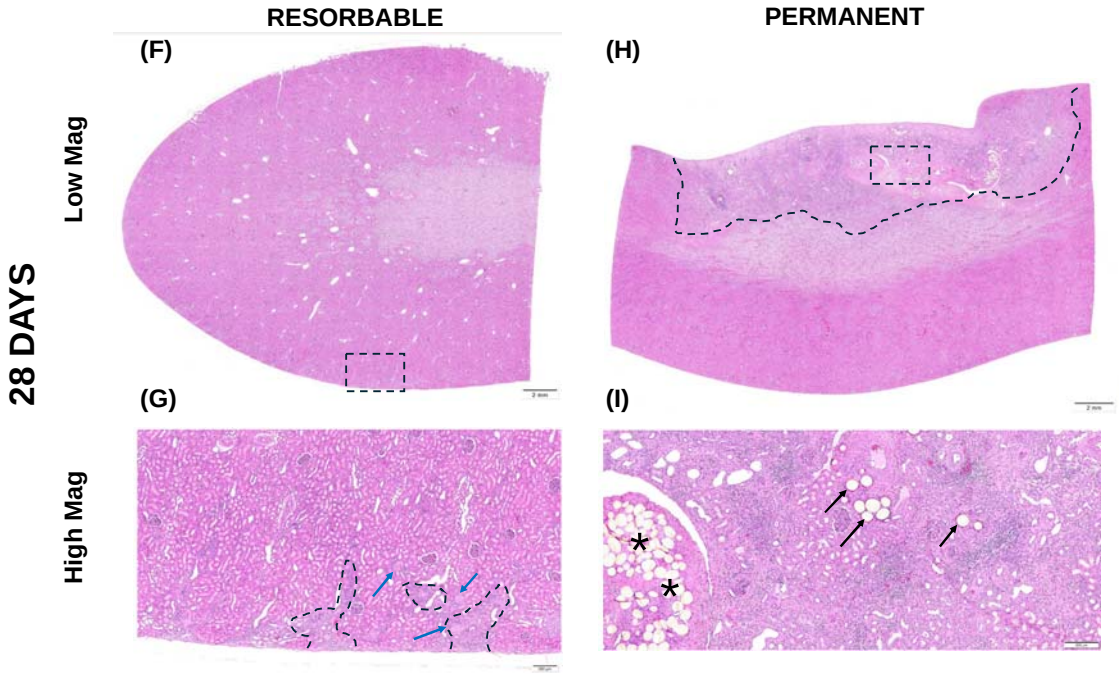

Figure 4 (F-I): (F) Low magnification view of a section of the right kidney treated with RM after 28 days; (G) Higher magnification image (scale bar 200 µm) of the box in (F) shows small areas of tubular degeneration/regeneration and interstitial fibrosis (dashed lines) and associated sclerotic glomeruli (blue arrows).(H) Low magnification view (scale bar 2mm) of the right kidney treated with PM after 28 days with extensive focus of cortical necrosis, fibrosis and inflammation indicated by the dashed line; (I) Magnified view (scale bar 200 µm) of the box in (H) demonstrates extensively disrupted and degenerative architecture with fibrosis and inflammation. Several isolated PM are indicated (arrows), and the vessel on the left contains a dense cluster (asterisks) of many PM with fibrin.

4 Discussion

Durability of the Occlusion

Amongst the resorbable embolic agents, the off-labelled IMP/CS antibiotics have been used successfully to date to treat MSK-associated pain.

We have previously reported on the angiographic assessment of the duration of occlusion for the SakuraBead RM in the porcine kidney, which showed almost complete restoration of flow in the target area within 1-2 hours post embolization [ref animal 1]. Moreover, it was observed that flow was restored in the artery by gradual proximal refilling of the vessels suggesting a progressive breakdown of the RM and migration downstream of smaller particulate fragments. This supposition is supported in the present study by the complete absence of any intact RM seen in the histology at 24 hours and by the detection of just a single 40 mm embolic fragment in the histological evaluation (Fig. 4 (A-B)) consistent with the bioerosion of the 200 mm alginate microspheres originally administered. The use of PM to embolize the renal arteries resulted in the expected durable occlusion with intact microspheres present within the tissue sections at all time points. Previous reports investigating the effects of Embozene PM in the porcine kidney model demonstrated 82.35% recanalization of the vessels at 4 weeks when embolized with 100 mm sized particles (Stampfl, Bellemann, et al., 2008). The investigators attribute recanalization post embolization with resorption of thrombus in the vessel (although a minor effect given the packing efficiency of small microspheres within the vessel lumen) and more predominantly neoangiogenesis. In this study by Day 28 thrombus in the vessels had resolved (Fig. 3(A)) and numerous PM remained present embedded within the reorganised tissue in the vessel lumen. The presence of neovascularization was confirmed at this timepoint Fig. 3(B), although high degrees of recanalization were not as evident as in the previous study, which

could be a result of differences in the amount of embolic administered between their study and ours.

Tissue Responses

After up to 28 days in the porcine renal artery embolization model, administration of RM was associated with no local or systemic adverse responses. Evidence of RM was only rarely suspected at 24 hours, with foci being uncommon, and extremely inconspicuous; renal tissue responses were minimal and indicative of dispersed, minute areas of ischemic injury. The vast majority of the RM material appears to have broken down is no longer evident in the vasculature. Studies conducted on the *in vivo* fate of radiolabelled alginate has shown that once the polysaccharide chains have been degraded into fragments of molecular weight ≤ 48 kDa, they are excreted in the urine within 24 hours and hence do not accumulate within the body (Duncan (Al-Shamkhani A et al.,). This is consistent with our reported results on *in vitro* RM degradation which demonstrated that the alginate microspheres were broken down into fragments lower than the renal clearance threshold in less than two hours [ref animal 1].

The PM were associated with readily apparent regionally extensive, localized regions of transcortical infarction, with abundant intraarterial microspheres present across time points, as observed previously for this type of product (Stampfl, Bellemann, et al., 2008). There was no arterial luminal occlusion in the RM group while maximum luminal occlusion in the PM group was marked across time points. Vascular injury in the RM group was restricted to rare medial involvement at 24 hours and was absent at all subsequent time points. Maximum vascular injury in the PM group generally extended to tunica media or EEL/adventitia regardless of time point. Renal parenchymal necrosis in the RM group through Day 3 was occasional and minimal, and necrosis was absent at later time points. In the PM group renal cortical necrosis was universally present across time points, being widespread and marked through Day 3 and then decreased to moderate at Day 7 and mild at Day 28. Tubular epithelial degeneration/regeneration was minimal in the RM groups across time points while it was moderate in the PM groups by Days 7 and 28. Hemorrhage was absent with the RM group, while in the PM group it was moderate through Day 3 and subsequently decreased. Fibroplasia (i.e., presence of reactive fibroblasts as part of a subacute to chronic response) was absent or nearly so in the RM group, while in the Control

group it was mild by Day 7. Fibrosis (i.e., presence of mature collagen as part of a chronic tissue response) was minimal-mild or lower in the RM group, while in the PM group it was moderate by Day 28. Macroscopic observations at necropsy, related to treatment, were consistent and notable in the PM group, exhibiting regionally extensive bilateral, acute to chronic renal infarction. Findings in the RM group were absent to mild. There was no gross or histologic evidence of systemic tissue responses in either RM or PM groups, nor was there premature mortality associated with the conduct of this study, indicating that embolization with either RM or PM is a safe procedure when conducted properly. The differences in tissue responses observed between the RM and PM are therefore due to the extent of the ischemic insult postembolization of the vessel, with only minor effects observed after RM administration, whilst use of PM induces significant tissue changes and ensuing necrosis that requires a longer period of healing

Inflammatory Response and Neoangiogenesis

There was no treatment material-associated inflammation in the RM group, regardless of time point, consistent with a transient ischemic intervention (Fig. 3(C)). The rare material foci observed at 24 hours showed no associated inflammatory reaction, indicative of a highly biocompatible material. It is also intriguing however, that anti-inflammatory properties of alginate oligosaccharide breakdown products have been reported in the literature (Hao et al., 2023), although this cannot be substantiated by the scant observations made in this study.

The PM material-associated inflammation was minimal or minimal-mild across time points and was characteristic of a classic foreign body reaction. Neutrophils were predominant through Day 3 and macrophages and giant cells at Days 7 and 28 (Fig. 3(C)). This is somewhat contradictory to the findings of Stampfl *et al*, who reported the absence of inflammation at 4 weeks postembolization (Stampfl, Bellemann, et al., 2008), attributing this to the highly biocompatible nature of the hydrogel material and its Polyzene-F coating (Stampfl, Stampfl, et al., 2008). The reasons for the observed differences are unclear but could be related to the amount of embolic delivered and hence the extent of the ischemic injury experienced. A high degree of tissue damage will create a more severe inflammatory response and those inflammatory cells that are recruited to the target site are more likely to remain associated with any foreign material that remains in the weeks following the injury.

There was evidence of neovascularization for the PM group at Day 28 (Fig. 3(B)), a commonly observed phenomenon following vascular remodelling in the occluded arteries and which can lead to vessel recanalization over time. Given that the objective of GAE is to destroy neovessels and associated neonerves that invade the cartilage space (Talaie et al., 2022), the occurrence of neovascularization following permanent occlusion of the genicular vessels would be an undesirable outcome. This supports the supposition for a milder, transient embolization of the target genicular arteries to allow flow in the main vessels to recover and limit the extent of local inflammation and vessel remodelling. Moreover, it has been shown that GAE performed using Embozene PM has a significantly higher ($P<0.00001$) minor complication rate compared to the resorbable IMP/CS (Torkian et al., 2021). Although technique and particle size no doubt have an influence on these complications, it is thought the permanent presence of Embozene PM in the vessels leads to increased transient cutaneous ischemia and skin discoloration and more significant postembolization syndrome symptoms.

Study Limitations

The main objectives of this study were to assess the safety and local tissue responses to embolization using a novel RM compared to an existing PM. The porcine renal embolization model was selected because of its widespread use in evaluating embolic materials and relevance of the size of the anatomy to that of a human. It does not, however, represent the vascular anatomy of the genicular arteries or the surrounding tissue types of the knee, the intended target site for the use of this novel resorbable temporary embolic agent. We will report in the future on results from GAE using RM in a novel porcine knee model of osteoarthritis [ref animal 3]. Based upon bench *in vitro* degradation measurements [ref animal 1], there was an expectation that the RM would breakdown over a 24 hour period and that more fragments of embolic material might be detectable at this time point. Degradation *in vivo* is evidently more efficient (most probably due to the content of ions in the blood and pulsatile nature of the flow) and it would have been useful in retrospect to include an earlier observation time point to better understand the aspect of the degradation RM in the histology evaluation.

Overall, embolization using SakuraBead RM is safe with no signs of adverse tissue responses that would be of concern for their use as a temporary occlusion agent for use in GAE.

Resorption occurs within a few hours with little sign of any residual material at 24 hours. Tissue injury is mild and with no evidence of any inflammatory response to the material. The behavior of the RM is therefore consistent with the requirements of an embolic suitable for GAE, being easily handled and administered, biocompatible and with a degradation time consistent with that of IMP/CS particles, hence positioning the RM as a viable alternative to the antibiotic combination which has concerns regarding allergic reactions in patients. A 15 patient First in Human study using the SakuraBead to reduce pain associated with knee osteoarthritis is currently in progress for which the first results will be reported in due course.

ACKNOWLEDGEMENTS

Acknowledgement This study was co-funded by the European Union and Enterprise-Ireland DTIF grant. Views and opinions expressed are however those of the authors only and do not necessarily reflect those of the European Union or European Innovation Council and SMEs Executive Agency (EISMEA). Neither the European Union nor EISMEA can be held responsible for them.

Conflict of Interest *statement* *Liam Farrissey reports financial support was provided by Disruptive Technologies Innovation Fund (Grant number: 174147), Enterprises Ireland. Liam Farrissey reports a relationship with CrannMed 43 Ltd that includes: board membership and employment. Liam and Sankalp inventors have patent #US 12083242 issued to CrannMed Ltd*

5 References

Al-Shamkhani A; Duncan R. (1995) Radioiodination of Alginate via Covalentlybound Tyrosineamide Allows Monitoring of Its Fate in Vivo. *J. Bioactive Compatible Polymers*, *10*, 4–13.

Barnett, B. P., Hughes, A. H., Lin, S., Arepally, A., & Gailloud, P. H. (2009). In Vitro Assessment of EmboGel and UltraGel Radiopaque Hydrogels for the Endovascular Treatment of Aneurysms. *Journal of Vascular and Interventional Radiology*, *20*(4), 507–512. https://doi.org/10.1016/j.jvir.2009.01.005

Becker, T. A., Kipke, D. R., & Brandon, T. (2000). Calcium alginate gel: A biocompatible and mechanically stable polymer for endovascular embolization, *Journal of Biomedical Materials Research: An Official Journal of The Society for Biomaterials and The Japanese Society for Biomaterials*, 54(1), 76-86.

Bhatia, S., Jalaeian, H., Kumar, J., Acharya, V., Shibuya, M., Bhatia, A., & Okuno, Y. (2023). Two-year outcomes comparing Embosphere® microspheres versus Imipenem Cilastatin for genicular artery embolization in patients with moderate to severe knee osteoarthritis. *Knee*, *41*, 38–47. https://doi.org/10.1016/j.knee.2022.12.008

Camacho, A., Ahn, E. H., Appel, E., Boos, J., Nguyen, Q., Justaniah, A. I., Faintuch, S., Ahmed, M., & Brook, O. R. (2019). Uterine Artery Embolization with Gelfoam for Acquired Symptomatic Uterine Arteriovenous Shunting. *Journal of Vascular and Interventional Radiology*, *30*(11), 1750–1758. https://doi.org/10.1016/j.jvir.2019.04.002

Choi, H., Choi, B., Yu, B., Li, W., Matsumoto, M. M., Harris, K. R., Lewandowski, R. J., Larson, A. C., Mouli, S. K., & Kim, D. H. (2021). On-demand degradable embolic microspheres for immediate restoration of blood flow during image-guided embolization procedures. *Biomaterials*, *265*. https://doi.org/10.1016/j.biomaterials.2020.120408

Doucet, J., Kiri, L., O'Connell, K., Kehoe, S., Lewandowski, R. J., Liu, D. M., Abraham, R. J., & Boyd, D. (2018). Advances in degradable embolic microspheres: A state of the art review. In *Journal of Functional Biomaterials*, 9(1). https://doi.org/10.3390/jfb9010014

Forster, R. E. J., Thürmer, F., Wallrapp, C., Lloyd, A. W., MacFarlane, W., Phillips, G. J., Boutrand, J. P., & Lewis, A. L. (2010). Characterisation of physico-mechanical properties and degradation potential of calcium alginate beads for use in embolisation. *Journal of Materials Science: Materials in Medicine*, *21*(7), 2243–2251. https://doi.org/10.1007/s10856-010-4080-y

Hao, Y., Fang, H., Yan, X., Shen, W., Liu, J., Han, P., Zhao, Y., Zhang, W., & Feng, Y. (2023). Alginate Oligosaccharides Repair Liver Injury by Improving Anti-Inflammatory Capacity in a Busulfan-Induced Mouse Model. *International Journal of Molecular Sciences*, *24*(4). https://doi.org/10.3390/ijms24043097

Jain, D., & Bar-Shalom, D. (2014). Alginate drug delivery systems: Application in context of pharmaceutical and biomedical research. *Drug Development and Industrial Pharmacy*, *40*(12), 1576–1584. https://doi.org/10.3109/03639045.2014.917657

Maeda, N., Verret, V., Moine, L., Bédouet, L., Louguet, S., Servais, E., Osuga, K., Tomiyama, N., Wassef, M., & Laurent, A. (2013). Targeting and recanalization after embolization with calibrated resorbable microspheres versus hand-cut gelatin sponge particles in a porcine kidney model. *Journal of Vascular and Interventional Radiology*, *24*(9), 1391–1398. https://doi.org/10.1016/j.jvir.2013.05.058

Okuno, Y., Korchi, A. M., Shinjo, T., & Kato, S. (2015). Transcatheter Arterial Embolization as a Treatment for Medial Knee Pain in Patients with Mild to Moderate Osteoarthritis. *CardioVascular and Interventional Radiology*, *38*(2), 336–343. https://doi.org/10.1007/s00270-014-0944-8

Owen, R. J., Nation, P. N., Polakowski, R., Biliske, J. A., Tiege, P. B., & Griffith, I. J. (2012). A preclinical study of the safety and efficacy of Occlusin™ 500 artificial embolization device in sheep. *CardioVascular and Interventional Radiology*, *35*(3), 636–644. https://doi.org/10.1007/s00270-011-0218-7

Pieper, C. C., Meyer, C., Vollmar, B., Hauenstein, K., Schild, H. H., & Wilhelm, K. E. (2015). Temporary Arterial Embolization of Liver Parenchyma with Degradable Starch Microspheres (EmboCept®S) in a Swine Model. *CardioVascular and Interventional Radiology*, *38*(2), 435–441. https://doi.org/10.1007/s00270-014-0966-2

Reig-Vano, B., Tylkowski, B., Montané, X., & Giamberini, M. (2021). Alginate-based hydrogels for cancer therapy and research. In *International Journal of Biological Macromolecules*, 170, 424–436). https://doi.org/10.1016/j.ijbiomac.2020.12.161

Schwarz, A., Zhang, H., Metcalfe, A., Salazkin, I., & Raymond, J. (2004). Transcatheter embolization using degradable crosslinked hydrogels. *Biomaterials*, *25*(21), 5209–5215. https://doi.org/10.1016/j.biomaterials.2003.12.022

Simó, G., Fernández□Fernández, E., Vila□Crespo, J., Ruipérez, V., & Rodríguez□Nogales, J. M. (2017). Research progress in coating techniques of alginate gel polymer for cell encapsulation. In *Carbohydrate Polymers*, Vol. 170, 1–14. https://doi.org/10.1016/j.carbpol.2017.04.013

Stampfl, S., Bellemann, N., Stampfl, U., Radeleff, B., Lopez-Benitez, R., Sommer, C. M., Thierjung, H., Berger, I., & Richter, G. M. (2008). Inflammation and Recanalization of Four Different Spherical Embolization Agents in the Porcine Kidney Model. *Journal of Vascular and Interventional Radiology*, *19*(4), 577–586. https://doi.org/10.1016/j.jvir.2008.01.011

Stampfl, S., Stampfl, U., Bellemann, N., Sommer, C. M., Thierjung, H., Radeleff, B., Lopez-Benitez, R., Berger, I., Kauffmann, G. W., & Richter, G. M. (2008). Biocompatibility

and recanalization characteristics of hydrogel microspheres with polyzene-F as polymer coating. *CardioVascular and Interventional Radiology*, *31*(4), 799–806. https://doi.org/10.1007/s00270-007-9268-2

Talaie, R., Torkian, P., Clayton, A., Wallace, S., Cheung, H., Chalian, M., & Golzarian, J. (2022). Emerging Targets for the Treatment of Osteoarthritis: New Investigational Methods to Identify Neo-Vessels as Possible Targets for Embolization. In *Diagnostics*, 12 (6), 1403. https://doi.org/10.3390/diagnostics12061403

Torkian, P., Golzarian, J., Chalian, M., Clayton, A., Rahimi-Dehgolan, S., Tabibian, E., & Talaie, R. (2021). Osteoarthritis-Related Knee Pain Treated With Genicular Artery Embolization: A Systematic Review and Meta-analysis. In *Orthopaedic Journal of Sports Medicine*, 9(7), 1-15. https://doi.org/10.1177/23259671211021356

Van Elk, M., Ozbakir, B., Barten-Rijbroek, A. D., Storm, G., Nijsen, F., Hennink, W. E., Vermonden, T., & Deckers, R. (2015). Alginate microspheres containing temperature sensitive liposomes (TSL) for MR-guided embolization and triggered release of doxorubicin. *PLoS ONE*, *10*(11), e0141626. https://doi.org/10.1371/journal.pone.0141626

Weng, L., Le, H. C., Talaie, R., & Golzarian, J. (2011). Bioresorbable hydrogel microspheres for transcatheter embolization: Preparation and in vitro evaluation. *Journal of Vascular and Interventional Radiology*, *22*(10), 1464-1470.e2. https://doi.org/10.1016/j.jvir.2011.06.010

Xie, Y., Gao, P., He, F., & Zhang, C. (2022). Application of Alginate-Based Hydrogels in Hemostasis. In *Gels*, 8(2), 109. https://doi.org/10.3390/gels8020109

Zeng, J., Li, L., Zhang, H., Li, J., Liu, L., Zhou, G., Du, Q., Zheng, C., & Yang, X. (2018). Radiopaque and uniform alginate microspheres loaded with tantalum nanoparticles for real-time imaging during transcatheter arterial embolization. *Theranostics*, *8*(17), 4591–4600. https://doi.org/10.7150/thno.27379

Zhang, H., Cheng, J., Ao, Q., Zhang, H., Cheng, J. Ao, Q., Rodríguez-Argüelles, C., & Simón-Vázquez, R. (2021). *Marine drugs Preparation of Alginate-Based Biomaterials and Their Applications in Biomedicine*. 19(5), 264. https://doi.org/10.3390/md

Zhang, M., & Zhao, X. (2020). Alginate hydrogel dressings for advanced wound management. In *International Journal of Biological Macromolecules*, Vol. 162, 1414–1428. https://doi.org/10.1016/j.ijbiomac.2020.07.311

Conflicts of interest statements